Prediction of diabetes mellitus development after kidney transplantation using patient-specific induced pluripotent stem cells

Sun Woo Lim
  Catholic University of Korea College of Medicine: Catholic University of Korea School of Medicine
Yoo Jin Shin
  Catholic University of Korea College of Medicine: Catholic University of Korea School of Medicine
Sheng Cui
  Catholic University of Korea College of Medicine: Catholic University of Korea School of Medicine
Eun Jeong Ko
  Catholic University of Korea College of Medicine: Catholic University of Korea School of Medicine
Byung Ha Chung
  Catholic University of Korea College of Medicine: Catholic University of Korea School of Medicine
Chul Woo Yang

  yangch@catholic.ac.kr

  Catholic University of Korea College of Medicine: Catholic University of Korea School of Medicine

Research Article

Abstract

Background: Multiple risk factors are involved in new-onset diabetes mellitus after transplantation; however, their prediction of clinical prognosis remains unclear. Therefore, we investigated whether patient-specific induced pluripotent stem cells (iPSCs) could help predict diabetes mellitus (DM) development before performing kidney transplantation (KT).

Methods: We first examined whole transcriptome and functional enrichment analyses of KT patient-derived iPSCs and revealed that insulin resistance, type 2 DM, and transforming growth factor-beta signaling pathways are associated between the group of DM and non-DM. We next determined whether the different genetic background was associated with development from iPSC into pancreatic progenitor (PP) cells.

Results: We found that the level of differentiation-related key markers of PP cells was significantly lower in the DM group than in the non-DM group. Moreover, the results of tacrolimus toxicity screening showed significant decrease in the number of PP cells of DM group compared with the non-DM group, suggesting that these cells are more susceptible to tacrolimus toxicity.

Conclusions: Taken together, the PP cells of the DM group showed low developmental potency, which was accompanied by a significantly different genetic background compared with the non-DM group. Thus, genetic analysis can be used to predict the risk of developing DM before performing KT.

Introduction

The incidence rate of new-onset diabetes after transplantation at 12 months posttransplant is 20–50% for kidney transplantation (KT). Diabetes mellitus (DM) after transplantation is associated with increased risks of graft rejection, infection, cardiovascular disease, and death [1–3]. Multiple risk factors have been implicated in DM development. Non-modifiable risk factors for new-onset DM include the following: advancing age; African American, Hispanic, or South Asian ethnicity; genetic background; positive family history of diabetes mellitus; polycystic kidney disease; and previously diagnosed glucose intolerance. Modifiable risk factors for new-onset DM after KT include the following: obesity; metabolic syndrome; hepatitis C virus or cytomegalovirus infection; and therapy with corticosteroids, calcineurin-inhibitor drugs (especially tacrolimus [Tac]), or sirolimus [4].

Emerging induced pluripotent stem cell (iPSC) technology can be expanded indefinitely to differentiate iPSCs into almost any organ-specific cell type. This technology would enable the generation of disease-relevant tissues from patients in scalable quantities. The use of patient-derived iPSCs has helped investigate the pathophysiological mechanism of development of disease. iPSC-derived organs and organoids are also currently being evaluated in regenerative therapy, which is proceeding toward clinical trials, and for disease modeling, which facilitates drug-screening efforts for discovering novel therapeutics [5, 6].

Therefore, we designed this study to investigate the feasibility of a novel diabetes mellitus (DM) prediction model involving patient iPSC cells. We reprogrammed the patient specific iPSC from peripheral blood mononuclear cell (PBMC) before performing KT. After about 1 year of KT, we selected the DM and non-DM group. First, we compared the genetic different between the DM and non-DM group by measuring RNA-sequencing analysis to reveal genetic link with insufficient pancreatic beta cell function or maturation.

Accumulating evidence indicates that pancreatic progenitor (PP) cells, which are multipotent cells with the potential to give rise to endocrine, exocrine, and epithelial cells, provide a powerful model system for examining the molecular characteristics of differentiating fetal-like pancreatic cells and for genetic analysis of pancreatic disease [7–9]. Therefore, we next compared the differentiation potential of PP cells between the DM and non-DM group by measuring morphology and differentiation marker expression.

Third, to determine whether the DM group after KT are likely to be susceptible to immunosuppressive agent, we tested the cell viability and insulin expression of PP cells from the DM and non-DM group during Tac-induced toxicity. Our results showed that the PP cells of the DM group showed low developmental potency, which was accompanied by a significantly different genetic background compared with the non-DM group. We expect that the results of our study will provide a rationale for the application for the prediction the risk of developing DM.

Materials And Methods

Study population

The Institutional Review Board (IRB) of the Catholic University of Korea, Seoul St. Mary's Hospital, approved this study (IRB number: KC16TISI0774). We recruited pre-KT patients ($n = 20$) who had never been treated with anti-diabetes medications and banked their PBMCs for further experiments. Of these, five patients were diagnosed with DM 1 year after KT; we selected matched patients with DM ($n = 4$) and non-DM individuals ($n = 4$) on the basis of the clinical index (Tables S1 and S2).

iPSC differentiation

iPSCs from four patients with DM and four non-DM individuals were generated using PBMCs, as previously described [10]. Briefly, the PBMCs obtained from each group were cultured for 4 days) at 37°C in an incubator with 5% CO_2 in StemSpan medium (09650; STEMCELL Technologies, Vancouver, Canada), which includes StemSpan CC100 (02690; STEMCELL Technologies), to expand CD34-positive cells. The expanded PBMCs were transfected using the CytoTune-iPS Sendai Reprogramming Kit (A16517; Life Technologies, Carlsbad, CA, USA), which includes the Yamanaka factors (Oct4, Sox2, KLF4, and c-Myc). PBMCs were induced to form iPSCs via centrifugation, and the resultant attached cells were expanded and purified by colony picking.

PP cell differentiation

Human iPSCs were subcultured in dishes coated with Matrigel (354277; Corning Life Sciences, Bedford, MA, USA) at 37°C in an incubator with 5% CO_2. Fresh mTeSR1 medium (05850; STEMCELL Technologies), which was replaced once per day, was used as the culture medium. iPSCs were split using trypsin– ethylenediaminetetraacetic acid (TE) (15400054; Life Technologies) at 70% confluence, and 10 μM of a rho-associated kinase (ROCK) inhibitor (1254; TOCRIS Bioscience, Bristol, UK) was added to the newly passaged cells. The STEMdiff pancreatic progenitor kit (05120; STEMCELL Technologies) was used as the culture medium for differentiation into PP cells.

Cell counting kit (CCK)-8 assay

iPSC-derived PP cells were differentiated in 96-well microplates for the CCK-8 assay. After differentiation, the cells were subjected to various Tac treatments for specified durations. CCK-8 solution (CK04-01; Dojindo Molecular Technologies, Kumamoto, Japan) was added to each well for 2 h. Subsequently, absorbance was measured at 450 nm using a VersaMax ELISA Reader (Molecular Devices, Sunnyvale, CA, USA).

Quantitative real-time (qRT)-polymerase chain reaction (PCR)

RNA was extracted from iPSCs or PP cells using RNA-Bee (CD-105B; Tel-Test, Friendswood, TX, USA), as per the manufacturer's instructions. First-strand cDNA was synthesized and subjected to qRT-PCR performed using SYBR Green Master Mix (DYRT1200; Dyne Bio Inc, Seongnam-si, South Korea) in a LightCycler 480 system (Roche, Basel, Switzerland). Target gene expression was normalized to glyceraldehyde 3-phosphate dehydrogenase (GAPDH) expression using the change-in-threshold method. Primer sequences are listed in Table S3.

Flow cytometry

iPSCs or iPSC-derived PP cells were dissociated using TE (15400054; Life Technologies). The cells were washed twice with FACS buffer (phosphate-buffered saline [PBS] containing 1% bovine serum albumin and 10 mM sodium azide), permeabilized for 30 min using flow cytometry fixation and permeabilization solution (554714; BD Biosciences, San Jose, CA, USA), washed with wash buffer, stained with anti-OCT3/4 (60093AD.1; STEMCELL Technologies) and anti-insulin (565689; BD Biosciences) antibodies for 1 h each, and then washed with FACS buffer. Subsequent analysis was performed using a BD LSRFortessa cell analyzer (BD Biosciences). Next, the data obtained were analyzed using the FlowJo V10 Single Cell Analysis Software (TreeStar Inc., OR, USA).

Suspension culture of PP cells

For further maturation of PP cells, suspension culture of PP cells was performed as previously described [11]. The PP cells were treated with 5 mg/mL dispase (07913; STEMCELL Technologies) for 5 min, followed by gentle pipetting to obtain cell clumps (< 100 μm). The cell clusters were transferred into a polystyrene 125 mL Spinner Flask (3152; Corning Life Sciences) and spun at 80–100 rpm overnight in suspension with DMEM-HG (10-017-CV; Corning Life Science) supplemented with 1 μmol/L ALK5

inhibitor II (ALX-270-445-M005; Enzo Life Sciences, Farmingdale, NY, USA), 100 ng/mL Noggin (6057-NG-100; R&D Systems, Minneapolis, MN, USA), and 1% B27 (17504077; Life Technologies).

Immunofluorescence staining

Cell clusters were obtained in 1.5 cc tubes after suspension culture for insulin staining. The cell clusters were then incubated with 4% paraformaldehyde for 15 min at 4'C and washed thrice in PBS in RT (room temperature). Subsequently, they were incubated with 0.1% Triton X-100 for 10 min and with 10% normal donkey serum for 1 h at RT. The primary antibodies, that is, anti-insulin (18–0067; Invitrogen, Camarillo, CA, USA), anti-OCT3/4 (5279; Santa Cruz Biotechnology, Santa Cruz, CA, USA), anti-SOX2 (365823; Santa Cruz Biotechnology), and anti-SSEA4 (MAB4304; Millipore Sigma, Burlington, MA, USA) antibodies, were incubated at 4°C overnight. On the next day, they were incubated with a secondary Cyanine3 (Cy3; Jackson ImmunoResearch, West Grove, PA, USA)-conjugated antibody for 2 h at RT. Subsequently, they were stained with 4',6-diamidine-2-phenylindole (DAPI; Vector Laboratories, Burlingame, CA, USA) for nucleic acid staining. Images were obtained using a Zeiss LSM700 confocal microscope (Carl Zeiss MicroImaging GmbH, Jena, Germany).

Electron microscopy (EM)

After the iPSCs differentiated into PP cells, the PP cells were fixed in 2.5% glutaraldehyde, 0.1 M phosphate buffer, and 1% O_SO_4 and then embedded in Epon 812. Ultrathin sections were cut, stained with uranyl acetate/lead citrate, and photographed under a JEM-1200EX transmission electron microscope (JEOL Ltd., Tokyo, Japan). The sections were randomly scanned at 20 different spots per sample at 5000× magnification.

Library preparation and sequencing

For control and test RNAs, library construction was performed using the QuantSeq 3' mRNA-Seq Library Prep Kit (Lexogen, Inc., Austria), according to the manufacturer's instructions. In brief, total RNA samples (500 ng each) were prepared, an oligo-dT primer containing an Illumina-compatible sequence at its 5' end was hybridized to the RNA, and reverse transcription was performed. After RNA template degradation, second-strand synthesis was initiated by a random primer containing an Illumina-compatible linker sequence at its 5' end. The double-stranded library was purified using magnetic beads to remove all reaction components. The library was amplified to add the complete adapter sequences required for cluster generation. The final library was purified from the PCR components. High-throughput sequencing was performed as single-end 75-bp sequencing using a NextSeq 500 system (Illumina, Inc., USA).

Data analysis

QuantSeq 3 mRNA-Seq reads were aligned using Bowtie2 [12]. Bowtie2 indices were either generated from the genome assembly sequence or the representative transcript sequences for alignment to the genome and transcriptome. The alignment file was used for assembling transcripts, estimating their abundance, and detecting differential gene expression. Differentially expressed genes (DEGs) were identified on the basis of counts from unique and multiple alignments by using coverage in BEDtools

[13]. The read count (RC) data were processed on the basis of the TMM + CPM normalization method by utilizing EdgeR within R (R development Core Team, 2020) using Bioconductor [14]. Gene classification was based on searches performed using the DAVID (http://david.abcc.ncifcrf.gov/) and Medline databases (https://www.ncbi.nlm.nih.gov/).

Statistical analyses

Data have been expressed in terms of mean ± standard error (SE) from at least three independent experiments. Multiple comparisons between groups were performed by one-way analysis of variance with the Bonferroni *post hoc* test using the Prism software (version 7.03 for Windows; GraphPad Software, La Jolla, CA, USA). Statistical significance was set at $P < 0.05$.

Results

Generation of iPSCs from PBMCs of pre-KT patients

PBMCs were induced to form iPSCs using Sendai viruses expressing Yamanaka factors (Oct4, Sox2, KLF4, and c-Myc). The reprogramming method was based on a previously described protocol involving serial centrifugation [10]. Colonies were generated from the somatic cells after approximately 18 days. PCR analysis of gene expression revealed that iPSCs expressed GAPDH, OCT3/4, SOX2, NANOG, LIN28, DPPA5, and TDGF1 (Fig. 1A). Flow cytometry revealed that approximately 90% of the iPSCs were positive for the pluripotency marker OCT3/4 (Fig. 1B). In addition, we confirmed the expression of the pluripotency markers OCT3/4, SOX2, SSEA4, KLF4, TRA-1-61, and TRA-1-81 at the protein level using immunofluorescence (Additional file 1: Fig. 1C, S1A). To confirm that the iPSCs generated were genomically normal, we analyzed their karyotypes using the GTG banding method. The iPSCs showed a normal karyotype of 44 + XX or 44 + XY, except in the case of DM 3 (trisomy 20) (Additional file 1: Fig. S1B).

Gene and functional enrichment analysis in patient-specific iPSCs of the DM group

To investigate the differences in the gene expression profiles of patient-specific iPSCs from the DM and non-DM groups, we performed transcriptomic analysis using RNA-seq. RNA-seq analysis was used to identify differentially expressed genes (DEGs) on the basis of the DM: non-DM ratio. A total of 242 DEGs with a P value of < 0.05 were identified, of which 187 genes showed two-fold upregulation and 55 genes showed two-fold downregulation (Fig. 2A). A volcano plot of the RNA-seq results illustrating the DEG findings with respect to the DM: non-DM ratio has been provided in Fig. 2B. On plotting the hierarchical clustering heat map of all DEGs, we found that most of these DEGs showed consistently higher or lower expression in individuals with DM (Fig. 2C).

Kyoto Encyclopedia of Genes and Genomes (KEGG) enrichment analysis was performed to predict the potential functions of these DEGs. The top 12 pathways are listed in Fig. 2D and E, and the 29 annotated

transcripts pertaining to these pathway terms are indicated in Table S4. Using qRT-PCR, we verified the validity of the annotated transcripts (Fig. 3A).

Differentiation of iPSCs into PP cells

To confirm differentiation of iPSCs into functional endocrine cells, we used a standardized simple protocol that helped confirm the expression of key markers, including PDX-1, NKX6.1, and SOX9, because insulin-secreting cells from iPSCs are difficult to cultivate in vitro. The protocol involved four stages over the course of 14 days of PP cell formation (Fig. 4A): definitive endoderm (end stage 1), primitive gut tube (end stage 2), posterior foregut endoderm (end stage 3), and PP cells (end stage 4). Representative images of cell morphological features (cell aggregation in high-density regions) at the end of each differentiation stage are shown in Fig. 4B.

Expression of differentiation markers for PP cells

We performed qRT-PCR for the differentiation markers (FOXA2, SOX17, GATA4, HNF1B, PDX-1, NKX6.1, SOX9, and NGN3) of PP cells in the DM and non-DM groups (Fig. 5). The mRNA expression of these genes in the DM group was significantly lower than that in the non-DM group (Fig. 4; FOXA2, 17.9 ± 2.2 vs. 54.9 ± 6.1; SOX17, 3.1 ± 0.7 vs. 9.5 ± 2.5; GATA4, 19.0 ± 13.3 vs. 125.4 ± 19.0; HNF1B, 27.8 ± 7.0 vs. 120.0 ± 26.2; PDX-1, 3.6 ± 0.4 vs. 8.3 ± 0.5; NKX6.1, 5.4 ± 0.5 vs. 123.3 ± 63.4; SOX9, 2.3 ± 0.4 vs. 10.8 ± 4.7; NGN3, 1.8 ± 0.2 vs. 5.5 ± 1.1; $P < 0.05$ vs. non-DM group).

Effect of Tac on insulin expression in patient iPSC-derived PP cells

Next, we confirmed the insulin levels in the PP cells from each group. Insulin protein and mRNA expression levels were confirmed via flow cytometry and qRT-PCR, respectively, performed using the differentiated PP cells, indicating that insulin expression in the DM group was significantly lower than that in the non-DM group (flow cytometry: 43 ± 7 vs. 66 ± 1, $P < 0.05$ vs. non-DM group; qRT-PCR, 1.6 ± 0.4 vs. 3.7 ± 0.5, $P < 0.05$ vs. non-DM group) (Fig. 6A, 6B and C). In addition, suspension cultures were performed for PP cells from each group for further maturation. Immunofluorescence results showed that insulin immunoreactivity was lower in the DM group than in the non-DM group (Fig. 7A and 7B). EM revealed that insulin granules were present in PP cells in the non-DM group but not in the DM group (Fig. 7C and 7D).

Effect of Tac on cell viability in patient iPSC-derived PP cells

We examined Tac-induced toxicity in PP cells. We differentiated the patient-specific iPSCs (non-DM individuals, $n = 4$; DM patients, $n = 4$) in a 96-well plate using the standardized protocol during the four stages over the 14-day course of PP cell formation. At the end of the differentiation stage, Tac was

administered for 24 h at serial doses of 0, 30, 40, 50, and 60 µg/mL, and toxicity was confirmed via a cell viability assay using CCK-8 (Fig. 8A). We calculated the area under the curve, indicating the individual cell viability rates at various Tac levels and exposure times (Fig. 8B).

The average cell viability results for each group are shown in Fig. 8C. In PP cells obtained from the DM group during Tac treatment, cell viability was significantly lower than that in the non-DM group when 40 and 50 µg/mL Tac was used (40 µg/mL Tac, 215 ± 5 vs. 271 ± 7, $P < 0.05$ vs. non-DM group; 50 µg/mL Tac, $P < 0.05$ vs. non-DM group). The insulin mRNA levels in the PP cells of the DM group were also markedly lower than those in the non-DM group when 50 µg/mL Tac was used (14 ± 3 vs. 50 ± 4, $P < 0.05$ vs. non-DM group) (Fig. 8D).

Discussion

Our current findings showed that KT patient-derived iPSC can be used to predict DM before performing KT. By whole transcriptome and functional enrichment analyses of KT patient-derived iPSCs, we found that insulin resistance, type 2 DM, and transforming growth factor-beta signaling pathways are associated between the group of DM and non-DM. The efficiency of differentiation of PP cells from iPSCs was lower in patients with DM than in non-DM individuals and that iPSC-derived PP cells in the insulin generation-related system are more vulnerable in patients with DM than in non-DM individuals. Moreover, tacrolimus toxicity screening showed significant decrease in the number of PP cells of DM group, suggesting that these cells are more susceptible to tacrolimus toxicity. Therefore, our results revealed a genetic link between insufficient maturation of iPSCs into the PP cells in the DM group.

We compared the reprogramming efficacy and pluripotency marker expression of the DM and non-DM groups. PBMCs were used as a platform for iPSC reprogramming because blood collection is less invasive than skin biopsy. For reprogramming, we used the Sendai virus transfection method. In the current study, we did not detect any differences in reprogramming efficacy or pluripotency marker expression between patients with DM and non-DM individuals. Thus, iPSCs from patients with DM have similar pluripotent potential as cells from non-DM individuals.

Next, we determined whether the differences of genetic background of the DM and non-DM groups, we performed RNA sequencing analysis using iPSCs. Using KEGG categories for the DM and non-DM groups, we performed functional and pathway enrichment analyses of DEGs. Among the 12 top-ranking listed pathways, we focused on insulin resistance and type 2 DM, which included the DEGs *SOCS3*, *MLXIPL*, *INSR*, *PPARA*, *PIK3R5*, and *SLC27A2*. We also found that the transforming growth factor (TGF)-beta signaling pathway was strongly associated with iPSCs in the DM group. On the basis of the in vitro protocol for differentiation of iPSCs into insulin-positive cells, including PP cells, inhibition of TGF-beta signaling using TGF-beta receptor antagonist, TGF-beta R1kinase inhibitor, and ALK5 inhibitor, is included in the protocols [7, 8, 11, 15, 16], suggesting that downregulation of TGF-beta signals is important during pancreatic development and beta cell maturation. Taken together, genetic alterations in patients with DM are likely to play an important role in diabetes onset after KT.

Based on the above result, we evaluated the efficacy of PP cell differentiation in both groups. During the differentiation into iPSC-PPs, we observed differences between the DM and non-DM groups in terms of differentiation efficacy. The iPSCs from the DM group consistently generated fewer PP cells than those from the non-DM group, and mRNA levels of PP cell differentiation-related genes from both groups using qRT-PCR. The number of insulin-positive cells and insulin mRNA expression levels were significantly lower in patients with DM than in non-DM individuals. Confocal microscopy and EM showed decreased insulin expression in patients with DM. These findings suggest that patient-derived iPSCs exhibit defective differentiation of disease-related cells and that PP cells show functional and morphologic defects in DM; therefore, PP cells can be used to predict DM.

Currently, there is lack of consensus regarding the preferred immunosuppression regimen to prevent DM, and individuals with DM are likely to be susceptible to immunosuppressive agents. Tac is the most popular mainstay for preventing transplant rejection, but little is known about the methods for predicting beta cell injury in individuals. Therefore, we tested Tac-induced toxicity in iPSCs and PP cells and compared cell survival rates and insulin expression. The PP cells of the DM group showed significantly lower cell viability and insulin mRNA expression than those of the non-DM group; such differences were not observed for the iPSCs (Additional file 1: Fig. S2). These findings demonstrate that PP cells derived from patients with DM are more vulnerable to Tac toxicity than those from non-DM individuals.

Our study has a few limitations. First, it included only a few individuals per group, which is insufficient for representing the overall new onset of diabetes scenario. Second, our study focused on Tac-induced DM; however, research involving other drugs, such as steroids, may also be required to evaluate DM. Third, potential target molecules need to be validated using inhibitors to confirm their functional roles.

Conclusions

We developed a novel approach for predicting DM before KT using patient-specific iPSCs. The model established in this study could be used to understand new onset of diabetes after KT pathophysiology and predict the risk of DM for developing novel therapeutics.

Abbreviations

CCK, cell counting kit; DEGs, differentially expressed genes; DM, diabetes mellitus; EM, electron microscopy; FACS, fluorescence-activated cell sorting; GAPDH, glyceraldehyde 3-phosphate dehydrogenase; iPSCs, induced pluripotent stem cells; IRB, Institutional Review Board; KEGG, Kyoto Encyclopedia of Genes and Genomes; KT, kidney transplantation; PP, pancreatic progenitor; PBMC, peripheral blood mononuclear cell; qRT-PCR, Quantitative real-time-polymerase chain reaction; RNA-seq, RNA sequencing; ROCK, rho-associated kinase

RT, room temperature; TE, trypsin− ethylenediaminetetraacetic acid.

Declarations

Acknowledgments

Not applicable.

Author contributions

SWL contributed to data collection, analysis, interpretation, and manuscript drafting. YJS, SC, EJK, BHC contributed to technical support and data collection. SWL and YJS contributed to data collection. SWL and CWY contributed to the study concept, interpretation, critical revision of the manuscript, and securing funding

Data availability statement

The data sets generated and/or analyzed during the current study are available from the corresponding author upon reasonable request.

Ethics approval and consent to participate

Our iPSCs are derived from human PBMC. The protocols were approved by the Institutional Review Board (IRB) of the Catholic University of Korea, Seoul St. Mary's Hospital (IRB number: KC16TISI0774).

Consent for publication

Not applicable

Competing interests

The authors declare that they have no completing interests.

Author details

[1]Convergent Research Consortium for Immunologic Disease, Seoul St. Mary's Hospital, College of Medicine, The Catholic University of Korea, Seoul, Republic of Korea. [2]Transplant Research Center, College of Medicine, The Catholic University of Korea, Seoul, Republic of Korea. [3]Division of Nephrology, Department of Internal Medicine, Seoul St. Mary's Hospital, College of Medicine, The Catholic University of Korea, Seoul, Republic of Korea.

References

1. Sulanc E, Lane JT, Puumala SE, Groggel GC, Wrenshall LE, Stevens RB. New-onset diabetes after kidney transplantation: an application of 2003 International Guidelines. Transplantation. 2005;80:945–52.

2. Kasiske BL, Snyder JJ, Gilbertson D, Matas AJ. Diabetes mellitus after kidney transplantation in the United States. Am J Transplant. 2003;3:178–85.

3. Chadban S. New-onset diabetes after transplantation–should it be a factor in choosing an immunosuppressant regimen for kidney transplant recipients. Nephrol Dial Transplant. 2008;23:1816–8.

4. Palepu S, Prasad GV. New-onset diabetes mellitus after kidney transplantation: Current status and future directions. World J Diabetes. 2015;6:445–55.

5. Wiegand C, Banerjee I. Recent advances in the applications of iPSC technology. Curr Opin Biotechnol. 2019;60:250–8.

6. Tang XY, Wu S, Wang D, Chu C, Hong Y, Tao M, et al. Human organoids in basic research and clinical applications. Signal Transduct Target Ther. 2022;7:168.

7. Rezania A, Bruin JE, Arora P, Rubin A, Batushansky I, Asadi A, et al. Reversal of diabetes with insulin-producing cells derived in vitro from human pluripotent stem cells. Nat Biotechnol. 2014;32:1121–33.

8. Pagliuca FW, Millman JR, Gürtler M, Segel M, Van Dervort A, Ryu JH, et al. Generation of functional human pancreatic β cells in vitro. Cell. 2014;159:428–39.

9. Jennings RE, Berry AA, Strutt JP, Gerrard DT, Hanley NA. Human pancreas development. Development. 2015;142:3126–37.

10. Kim Y, Rim YA, Yi H, Park N, Park SH, Ju JH. The Generation of Human Induced Pluripotent Stem Cells from Blood Cells: An Efficient Protocol Using Serial Plating of Reprogrammed Cells by Centrifugation. Stem Cells Int. 2016;2016:1329459.

11. Rezania A, Riedel MJ, Wideman RD, Karanu F, Ao Z, Warnock GL, et al. Production of functional glucagon-secreting α-cells from human embryonic stem cells. Diabetes. 2011;60:239–47.

12. Langmead B, Salzberg SL. Fast gapped-read alignment with Bowtie 2. Nat Methods. 2012;9:357–9.

13. Quinlan AR, Hall IM. BEDTools: a flexible suite of utilities for comparing genomic features. Bioinformatics. 2010;26:841–2.

14. Gentleman RC, Carey VJ, Bates DM, Bolstad B, Dettling M, Dudoit S, et al. Bioconductor: open software development for computational biology and bioinformatics. Genome Biol. 2004;5:R80.

15. Nostro MC, Sarangi F, Ogawa S, Holtzinger A, Corneo B, Li X, et al. Stage-specific signaling through TGFβ family members and WNT regulates patterning and pancreatic specification of human pluripotent stem cells. Development. 2011;138:861–71.

16. Schulz EC, Roth HM, Ankri S, Ficner R. Structure analysis of Entamoeba histolytica DNMT2 (EhMeth). PLoS ONE. 2012;7:e38728.
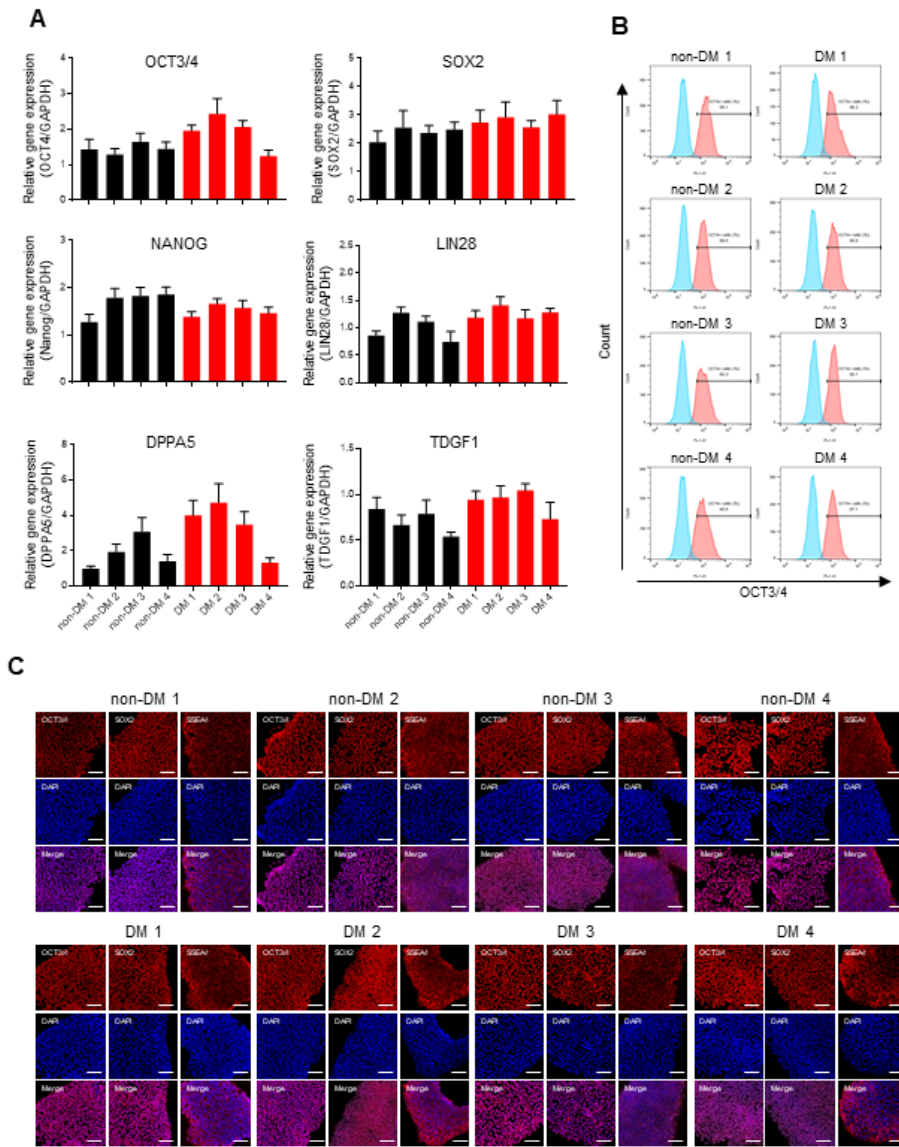
Figures

Fig. 1

Figure 1

iPSC generation from pre-KT patients without diabetes. (**A**) Quantitative real-time PCR data for pluripotency gene expression in iPSCs. (**B**) Flow cytometry data for iPSCs, showing an OCT4-positive cell population. (**C**) Immunocytochemistry images showing that pluripotency markers (OCT4, Sox2, and

SSEA4) were expressed in iPSCs. Data are represented as the mean ± SE values. Scale bar, 100 μm. DM, diabetes mellitus; PBMC, peripheral blood mononuclear cell; iPSC, induced pluripotent stem cell; PP, pancreatic progenitor; IS, immunosuppressant.

Fig. 2
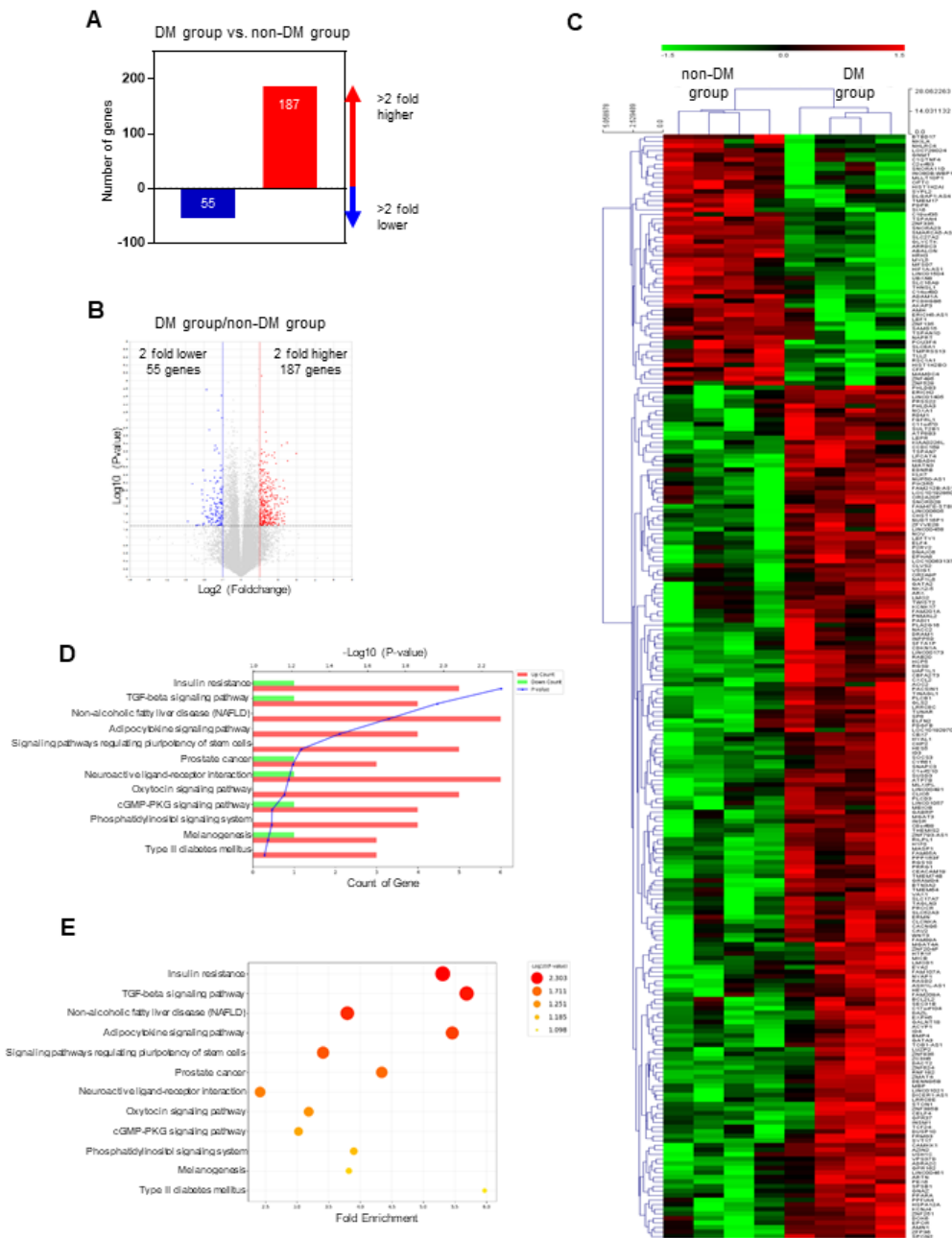
Figure 2

Differentially expressed gene (DEG) analysis with the DM:non-DM ratio. (**A**) Two-fold upregulated genes (187 genes) and two-fold downregulated genes (55). (**B**) Volcano plot showing the DEGs. The x-axis represents the log2 fold change conversion of the values, and the y-axis represents the significance value after $-\log 10$ conversion. Red dots indicate 187 upregulated DEGs, blue dots indicate 55 downregulated DEGs, and the gray area represents no DEGs. (**C**) Heat map showing the differential expression pattern of the DEGs. The color scale shows the gene expression values (log2fc). KEGG pathway analyses of DEGs and list of top 12 pathway by P values. (**D**) Bar graph represents up- and downregulated genes from the DEGs. Y-axis represents pathway name, and X-axis represents the number (count) of genes or -log10 (P value). (**E**) Size and color of each bubble represent the number of DEGs enriched in the pathway and -log10 (P value), respectively. Y-axis represents pathway name, and X-axis represents fold enrichment factor.
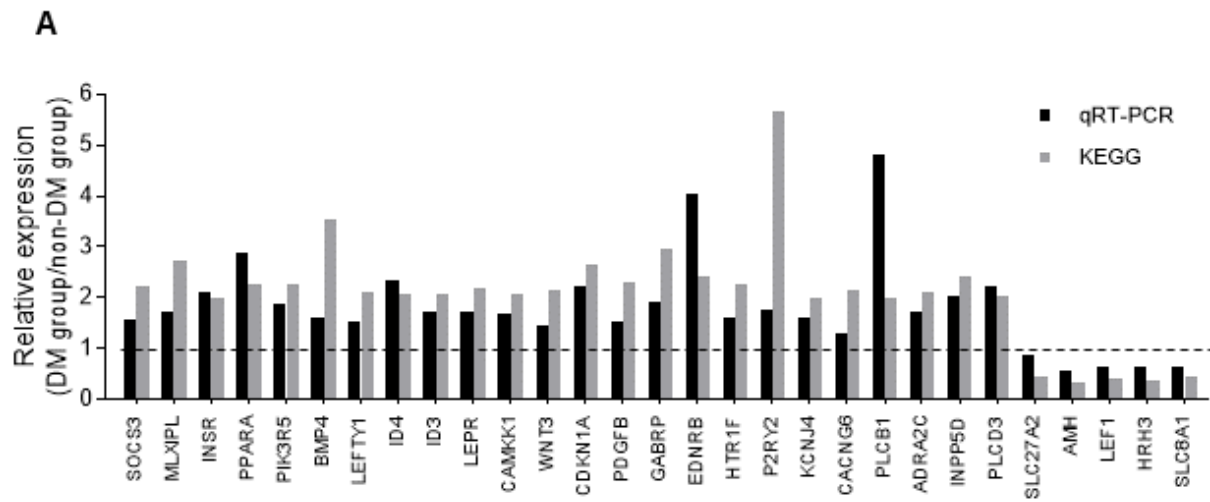
Fig. 3

A

Figure 3

Statistical comparison of KEGG pathways and validation of RNA-seq data by qRT-PCR. (**A**) RNA-seq− and qRT-PCR−based comparisons of the expression of select DEG target genes.
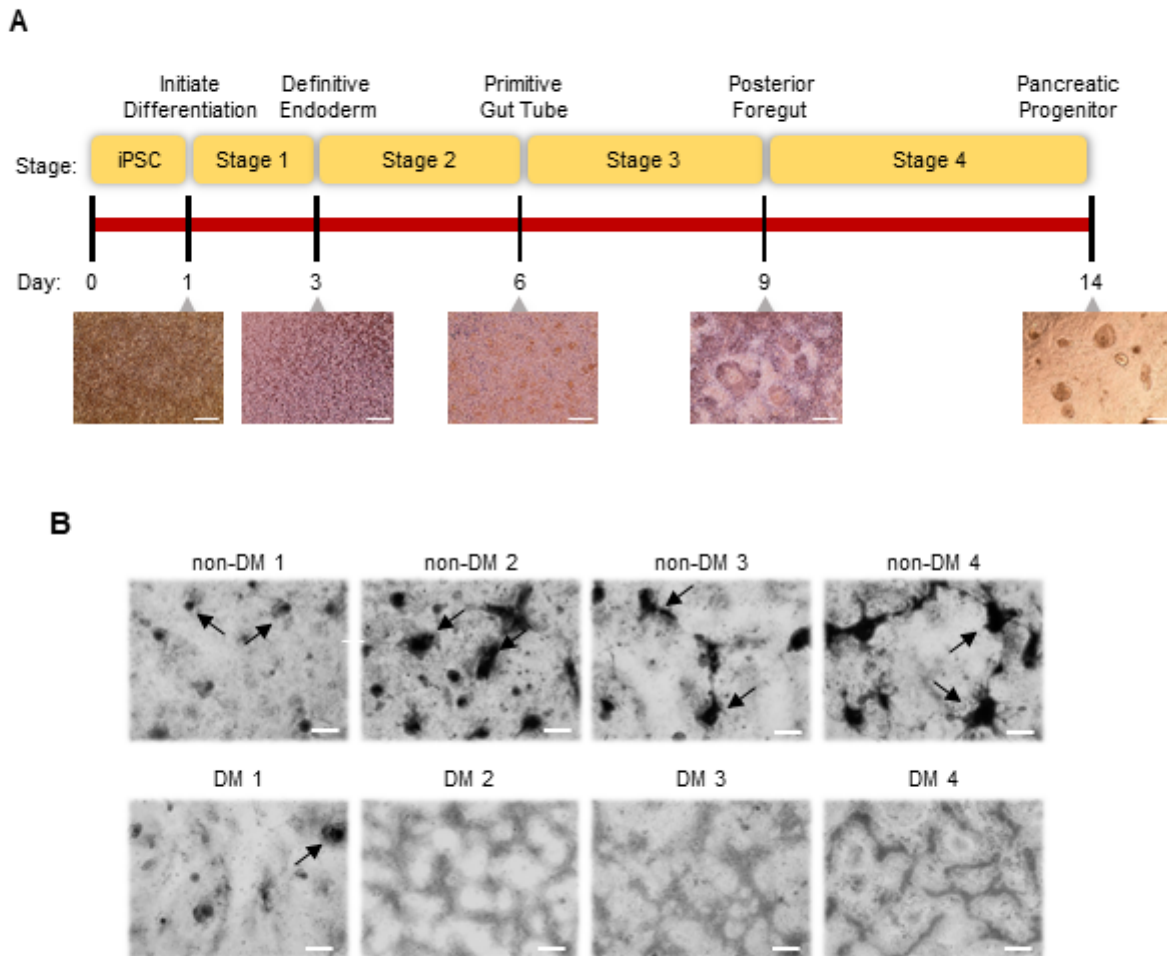
Fig. 4

A

| Stage: | iPSC | Stage 1 | Stage 2 | Stage 3 | Stage 4 |

Initiate Differentiation — Definitive Endoderm — Primitive Gut Tube — Posterior Foregut — Pancreatic Progenitor

Day: 0 1 3 6 9 14

B

non-DM 1   non-DM 2   non-DM 3   non-DM 4

DM 1   DM 2   DM 3   DM 4

Figure 4

Differentiation of iPSCs derived from patients with DM and non-DM individuals into pancreatic progenitor cells. (**A & B**) Overview of the differentiation protocol for 14 days and the cell morphological features at end stage 4 for the groups. Arrows in B indicate PP cell formation. Data are represented as the mean ± SE values. Scale bar, 250 μm in A and 200 μm in B. DM, diabetes mellitus.
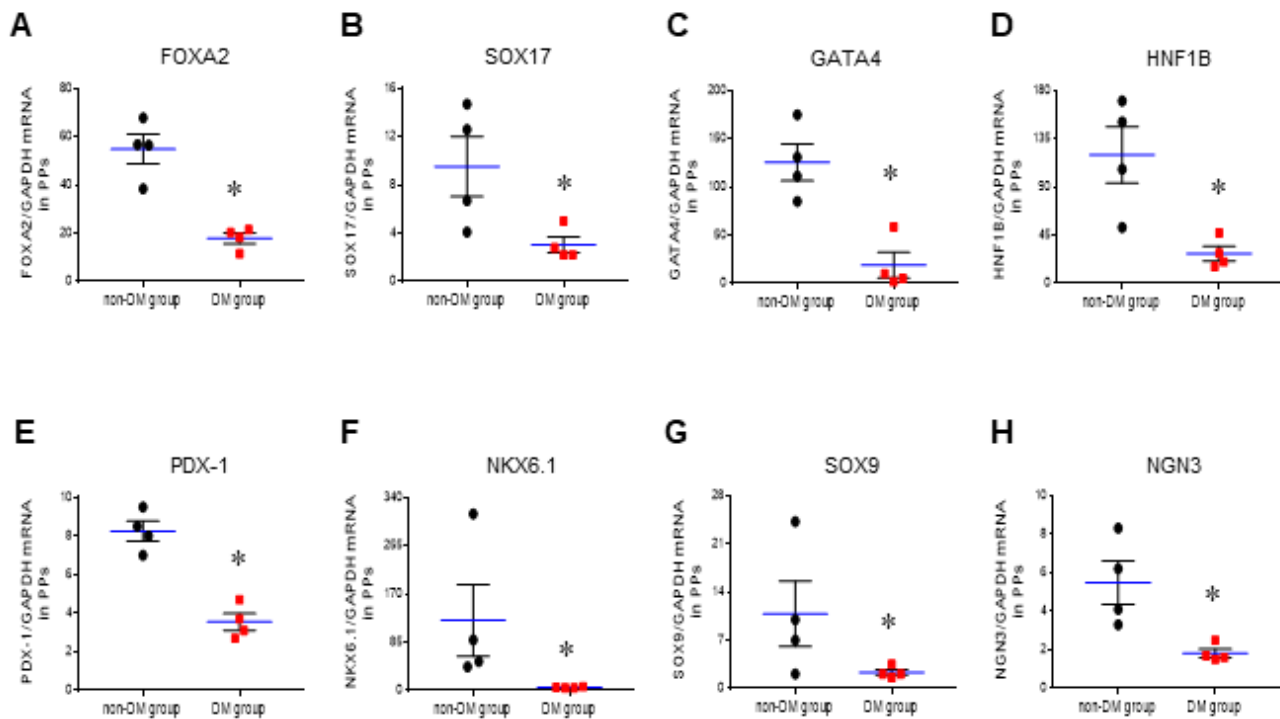
Fig. 5

Figure 5

mRNA expression levels of genes related to pancreatic beta cell function or differentiation, using real-time PCR analysis. iPSC-derived pancreatic progenitor (PP) cells from patients with DM and non-DM individuals. (**A**) *FOXA2*, (**B**) *SOX17*, (**C**) *GATA4*, (**D**) *HNF1B*, (**E**) *PDX-1*, (**F**) *NKX6.1*, (**G**) *SOX9*, and (**H**) *NGN3*. Data are represented as the mean ± SE values. *P < 0.05 vs. non-DM group. DM, diabetes mellitus.
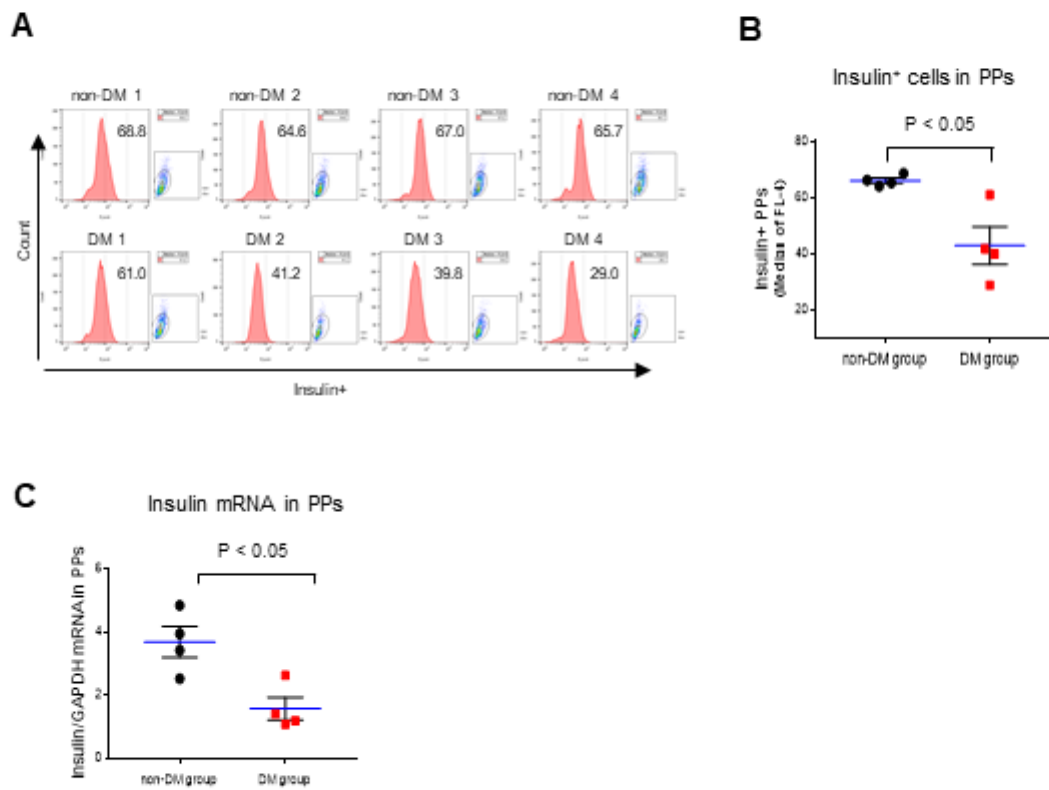
Fig. 6

Figure 6

Flow cytometry plots (**A**) and quantitative graphs (**B**) for insulin. (**C**) Insulin mRNA levels in iPSC-derived PP cells from patients with DM and non-DM individuals. Data are represented as the mean ± SE values. Scale bar, 250 μm in A and 200 μm in B. DM, diabetes mellitus.
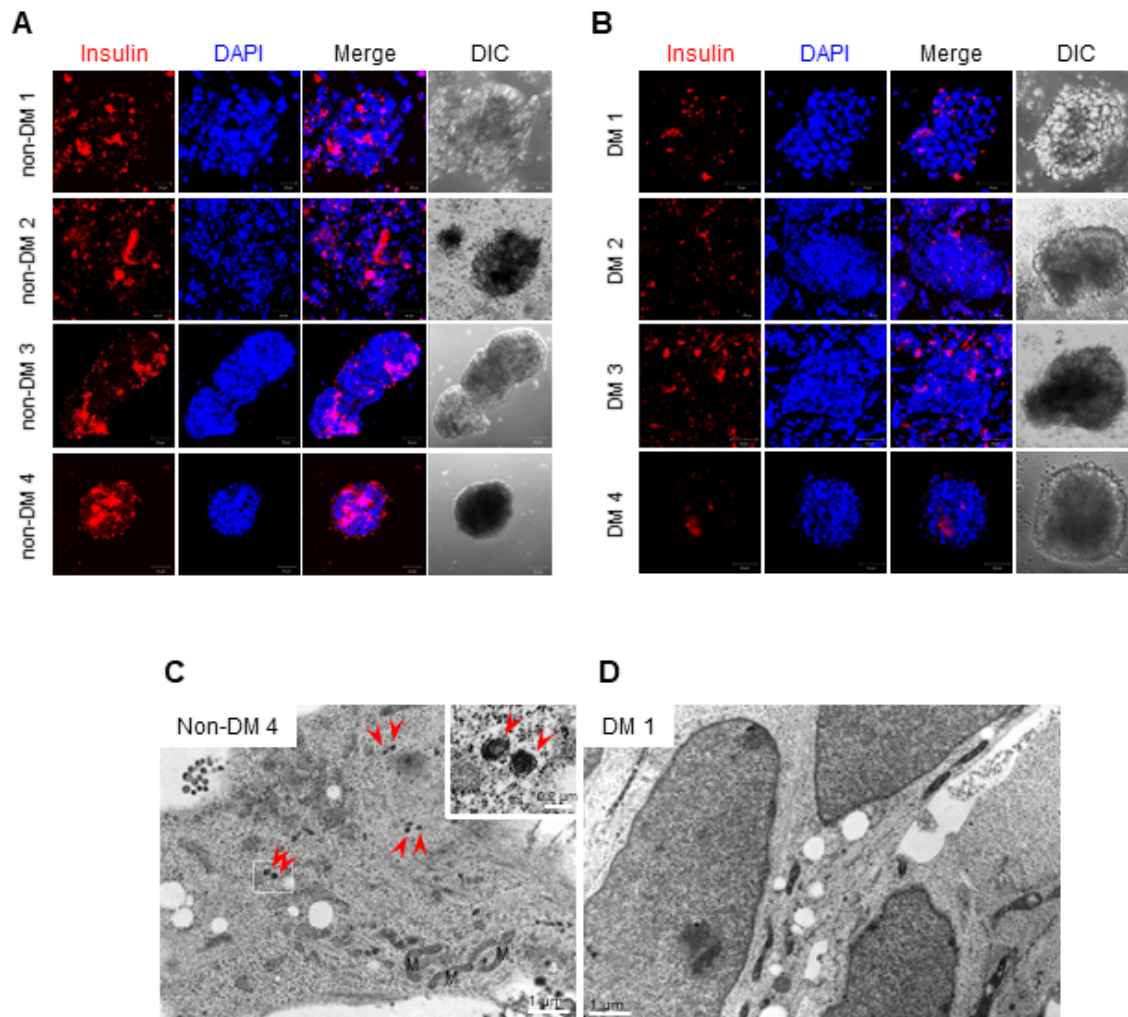
Fig. 7

Figure 7

Representative confocal microscopy images for insulin and transmission electron micrographs in iPSC-derived pancreatic progenitor (PP) cells from patients with DM and non-DM individuals. (**A** and **B**) PP cells were cultured under floating conditions for 1 day and were then collected for further immunocytochemistry analysis for insulin. (**C** and **D**) EM of iPSC-derived PP cells from patients with DM

and non-DM patients. Red arrows in C indicate insulin granules. Scale bar in A and B, 50 μm. M, mitochondria. DM, diabetes mellitus.
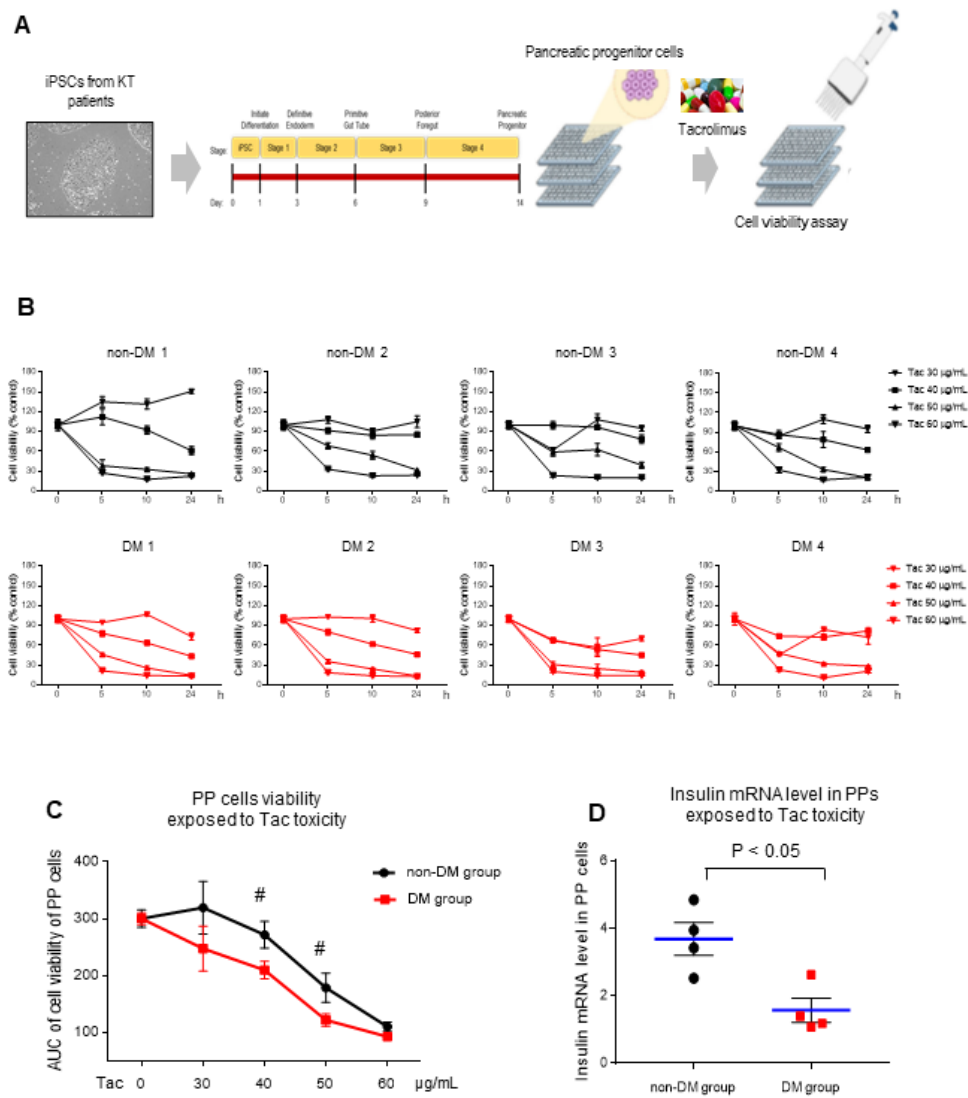
Fig. 8

Figure 8

Cell viability and insulin levels of iPSC-derived pancreatic progenitor (PP) cells from patients with DM and non-DM individuals during tacrolimus (Tac) treatment. (**A**) Scheme of cytotoxicity assay performed using

Tac-treated PP cells. (**B**) CCK-8 assay graphs of PP cells derived from iPSCs of patients with DM and non-DM individuals after incubation with different concentrations and for different exposure durations of Tac treatment. (**C**) Calculated area under the curve graphs from B graphs. (**D**) Insulin mRNA levels for PP cells from patients with DM and non-DM individuals treated with 50 μg/mL Tac. Data are represented as the mean ± SE values. [#]P < 0.05 vs. corresponding DM group. DM, diabetes mellitus.

Supplementary Files

This is a list of supplementary files associated with this preprint. Click to download.

- Finalver.Suppmaterials.docx
- FigS1.docx
- FigS2.docx
- TableS1.docx
- TableS2.docx
- TableS3.docx
- TableS4.docx